

Development of Deodorant Panel

M.Tajima, K.Nagano, M.Satao¹, R.Tano¹, H.Kitagawa² and Y.Noda²

Shimane Institute for Industrial Technology, 1 Hokuryo, Matsue, Shimane 690-0816, Japan

Fax: 81-852-60-5135, e-mail: tajima-masahiro@pref.shimane.jp

¹Kodama Co., Ltd., 1-3 Fujimi, Matsue, Shimaene 690-0026, Japan

Fax: 81-852-37-1134

²Department of Materials Science, Shimane University, 1060 Nishi-kawatsu, Matsue, Shimane 690-8504, Japan

Fax: 81-852-32-6319, e-mail: nodayasu@riko.shimane-u.ac.jp

A high efficient far-infrared light emitting panel was made using the recycled garnet sludge. The panel consists of plasma sprayed garnet layer and several catalysts. The catalytic actions of the hot panels were tested for removal of trace amounts of NH₃ or H₂S gas. At 300°C, catalytic decompositions of the gases were repeatedly observed as the decrease of residual amounts of the gases, while the layer with no catalyst caused no change in gas concentration. The exhausted heat was effectively utilized for thermoelectric generation using Bi-Te related modules. The results indicate that a multi-purposed panel heater has been developed with the functions of far-infrared emission, high deodorization and energy conservation.

Key words: plasma jet, deodorant catalyst, recycled garnet sludge, far-infrared light, thermoelectric generation

1. INTRODUCTION

Sealing of rooms in houses or buildings has recently become so tight that air ventilation is not made spontaneously. Thus, environmental degradation and healthy damage by bad smell gases or the volatile organic compounds (VOC) have been regarded as significant, and the apparatus which can remove these substances in the air has been developed. However, there are few simple heaters with the mixed deodorant function.

We investigated the re-using the sludge of garnet as a plasma-jet material, after the use as a polishing agent on water-jet cutting process [1]. Consequently, as for the garnet plasma jet panel, the efficient radiation property of far-infrared light was checked. Development was considered in the far-infrared heater of high-energy

efficiency using these characteristics.

In this study, we propose a deodorant panel with the complex functions. The far-infrared heater using the garnet plasma-jet film was produced with the deodorization catalyst [2]. The performances were examined to remove the bad smell and volatile organic compounds (VOC).

Furthermore, by using waste heat of the heater, power generation by the thermoelectric energy conversion was made. A panel with the complex functions with which circulation of indoor air was made by driving a fan and the performance of the generator was evaluated.

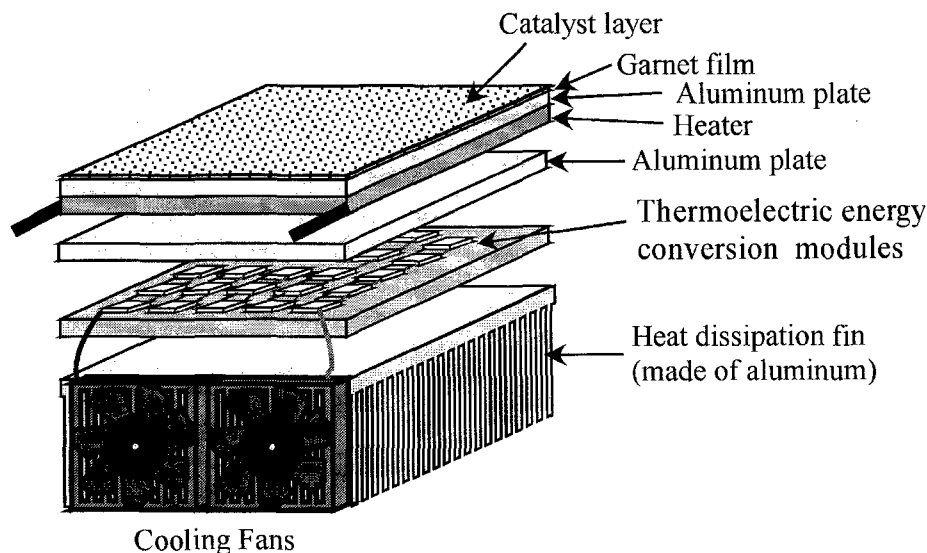


Fig. 1. Schematic drawing of the deodorant panel.

2. MANUFACTURING OF THE GARNET PLASMA JET PANEL

2.1 Formation of the deodorant catalyst

The garnet powder was ground and sieved into 45 to 75 μm in diameter. The garnet film of about 200 μm in thickness was deposited on the aluminum plate of 300 \times 300 \times 5 mm by plasma jet after the surface was treated by blast processing with the quartz sand of 20 meshes. Furthermore, the composition of MnO_2 : 10 wt% Cu-containing zeolite =1:1 was mixed with binder of 20 wt% alumina sol. The mixture was painted on the garnet layers with the density of about 0.4mg / mm^2 and then calcinated in air at 400 $^\circ\text{C}$ for 2 hours, resulting the formation of catalyst layer.

2.2 Construction of waste heat recovery system

In order to change the waste heat effectively into electricity on heating a catalyst layer, the power generation was made in which the Peltier modules and the heat dissipation fin was combined. It is useful to generate electricity with emitting heat of the fin to drive by using fans.

2.3 Composition of deodorant panel

The composition of the panel is shown in Fig.1. The aluminum plate where the catalyst is applied on the garnet film, a heater, and a thermoelectric energy conversion module, and a fin made of aluminum are piled up in order. Two fans are attached to the fin, where the fin radiates heat by the ventilation with the fan, which is also useful to circulate indoor warm air.

3. THE DEODORIZATION EFFECT

3.1 Adsorption performance

In the preliminary experiments, the bad smell gas concentration of ammonia or hydrogen sulfide did not decrease by using the simple garnet film before catalyst processing. The adsorption and decomposition of the gases by the catalyst layers were measured in 0.01 m^3 Teflon bag, 0.21 and 0.5 m^3 containers. After keeping the panel at a specified temperature, the bad smell gas of 10ppm was introduced into the container. After introducing the gas, the concentration of the residual gas was measured with the gas detection pipe at 10 to 180 min.

3.2 Deodorant characteristics

Figure 2 shows plots of gas concentration versus time measured at 25 $^\circ\text{C}$ for ammonia or hydrogen sulfide gas in the 0.01 m^3 Teflon bag. It is shown that gas concentration rapidly decreases and that the catalyst processing enhances the gas adsorptions.

In Fig. 3, the ammonia gas concentration is investigated at 300 $^\circ\text{C}$ after the repeated gas introductions, where the decrease of ammonia gas concentration is repeatedly observed, indicating stable activity of the catalyst [3].

After the tests at several temperatures, ammonia gas concentration is plotted versus time as shown in Fig. 4. As for the concentration, a detectable decrease is observed at 170 $^\circ\text{C}$. At 243 $^\circ\text{C}$, the rapid decrease of the concentration is found. Furthermore, in the successive measurement at 148 $^\circ\text{C}$, the deodorization effect became small. The catalyst effects have been ascribed to the

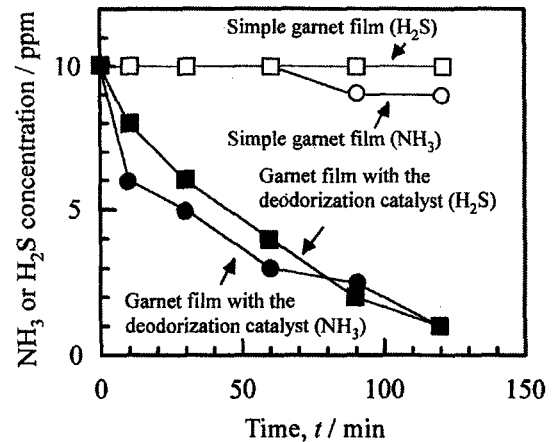


Fig. 2. Adsorption of ammonia or hydrogen sulfide gas. Plots of gas concentration versus time measured at 25 $^\circ\text{C}$ in the 0.01 m^3 Teflon bag.

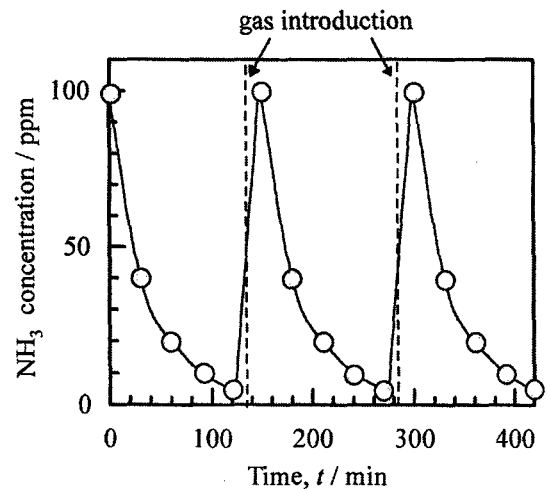


Fig. 3. Removal of ammonia gas. Plots of residual gas concentration after repeated introductions measured at 300 $^\circ\text{C}$ in the 0.21 m^3 container.

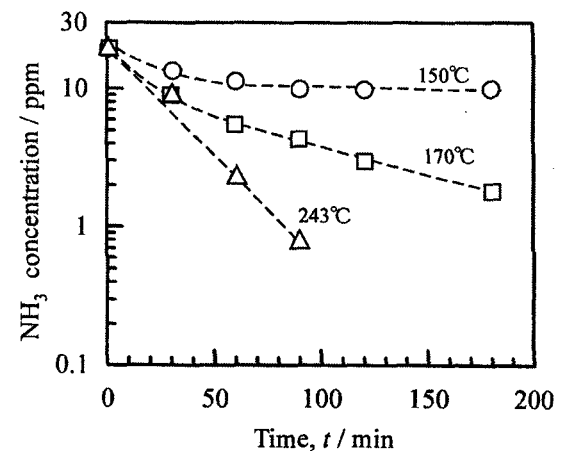


Fig. 4. Removal of ammonia gas. Plots of residual gas concentration versus time at different temperatures in the 0.5 m^3 container.

strong oxidation characteristics [3] of MnO_2 and Cu zeolite for NH_3 producing NO_3^- ion. [4] The deodorization in this study is attributable to the catalysis effect.

3.3 Far-infrared radiation characteristics

One of characteristics of garnet film exists in radiation of far-infrared light. The spectrum is measured for the panel which has the additional catalyst activity in the present study. The result in Fig.5 shows the efficient far-infrared radiation as well as garnet.

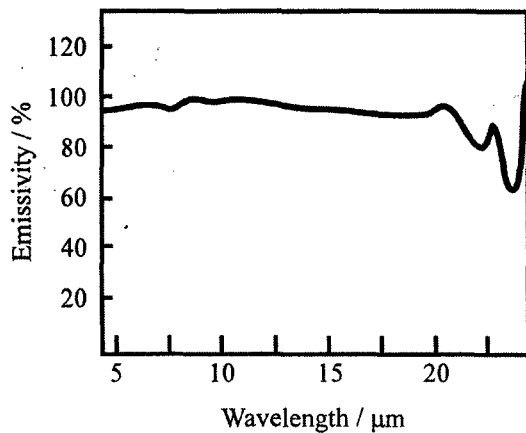


Fig. 5 Far-infrared radiation from the catalyst-garnet complex layer.

4. THERMOELECTRIC POWER GENERATION

4.1 Thermoelectric power generator

The deodorant panel shown in Fig.1 is obtained where the catalyst works well in the temperature $50 \sim 250^\circ\text{C}$. If electricity can be generated by using the waste heat, the cooling fan or ventilation can be operated. Such a deodorant panel surely is the product which fitted energy conservation and the environment friendly problem. In case of useful utilization of the waste heat in this temperature range, the thermoelectric power generation system is known to be most suitable where the solid-state module can be operated. The thermoelectric modules installed in the lower part of a deodorant panel and the fan is operated using the generated electricity. The output power of the thermoelectric generator was evaluated in temperature region of the deodorant panel operation.

4.2 Output power evaluation

The thermoelectric generator consists of 24 Bi-Te related modules (S.T.S. Co., 40×40 mm in size, 112 thermocouples/modules) which are connected in series. In the output measurement, the circuit which connected the ammeter and the load with the generator in series as shown in Fig. 6. The electronic load equipment (Takasago Manufacturing Co.) was used for the load and the output voltage measurement. The upper end (high temperature junction, T_h) of a thermoelectric modules was heated at 100, 120, 140, and 160°C by the heater, and the lower end (low-temperature junction, T_c) was

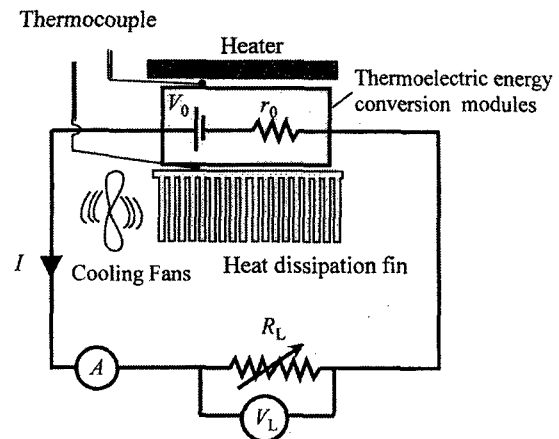


Fig. 6. Schematic diagram of the output measurement for thermoelectric generator.

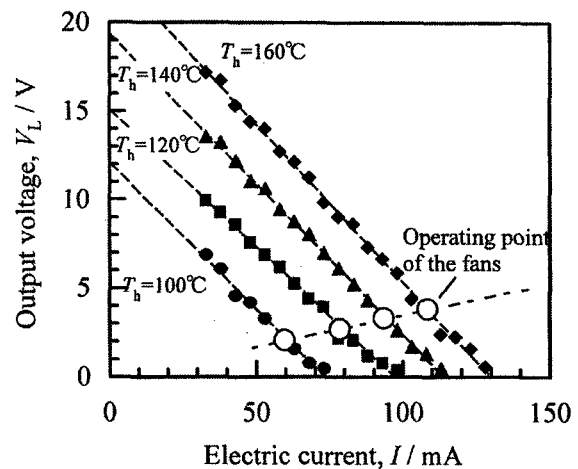


Fig. 7. Relationship between current I and output voltage V_L for the output measurement.

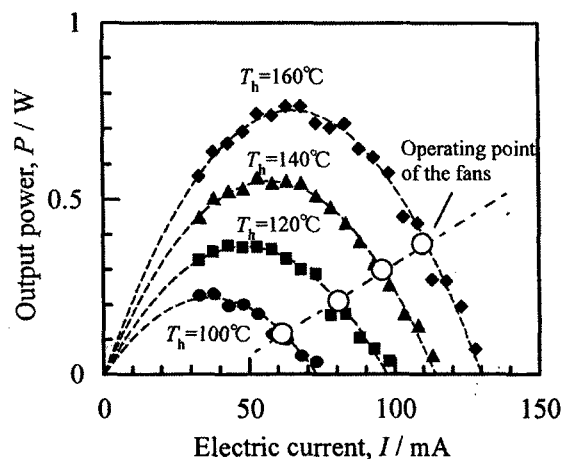


Fig. 8. Relationship between current I and the output power P for thermoelectric generator.

kept at about 40°C by the heat dissipation fin and the air cooling fan. Temperature difference $\Delta T = T_h - T_c$ was 60, 80, 100, and 120°C for the high temperature junction at $T_h = 100, 120, 140,$ and 160°C , respectively.

Under the these conditions, the current I which flows in a circuit was controlled from 33 up to 128 mA by changing the electronic load and then the output voltage V_L was measured. The relation between I and V_L , is given by the equation (1) using the open-circuit voltage V_0 and the internal resistance of the generator r_0 .

$$V_L = V_0 - r_0 I \quad (1)$$

When the upper end temperature T_h and the temperature difference ΔT are being fixed, it is possible that V_0 and r_0 are constants. By using eq. (1), the output power $P = I \cdot V_L$ is expressed as follows,

$$P = r_0 (I - V_0/2 r_0)^2 + V_0^2/4 r_0 \quad (2)$$

P is expressed as a function of I in eq.(2), and the maximum output is given by $P_{\max} = V_0^2/4 r_0$ at $I = V_0/2 r_0$.

4.3 Output power measurement

The relation between current I and output voltage V_L is shown in Fig. 7. Output voltage increases in proportion to the temperature difference, and decreases linearly with the increasing current for all the conditions. The dotted lines show the best fitted straight lines by the least-squares method. Using eq. (1), the V_0 and r_0 values are estimated and listed in Table 1.

The output power estimated using the V_0 and r_0 values are well reproducing the experiment value as shown by the dotted curves in Fig.8.

The current and the output power at which the maximum output is obtained become large with an increase of the temperature T_h . Moreover, the open circles in Fig. 7 and 8 show are operating points of the fan (inner resistivity: $35\Omega/2\text{fans}$) used for cooling or ventilation. It turns out that the fan can be operated with the increased power when the T_h and ΔT values increase, but not with the maximum power.

Table 1 Thermal condition, open-circuit V_0 , internal resistance r_0 , and the maximum power P_{\max} for thermoelectric generator.

| T_h (°C) | ΔT (°C) | V_0 (V) | r_0 (Ω) | P_{\max} (mW) |
|------------|-----------------|-----------|--------------------|-----------------|
| 100 | 60 | 12.1 | 165.6 | 221 (at 37mA) |
| 120 | 80 | 15.1 | 155.7 | 366 (at 48mA) |
| 140 | 100 | 19.4 | 169.9 | 554 (at 57mA) |
| 160 | 120 | 23.2 | 178.4 | 754 (at 65mA) |

References

- [1] M.Kantha Babu, O.V.Krishnaiah Chetty : Wear, 254, 763-773 (2003),.
- [2] T.Sadakata: Jpn. Kokai Tokkyo Koho 94,254,140, Sept. 13, (1994).
- [3] Lu Gang, B.G.Anderson, J.van Grondelle, R.A.van Santen: Catalysis Today, 61, 179-185 (2000).
- [4] Z.Schay, L.Guczzi, A.Beck, I.Nagy, V.Samuel, S.P.Mirajkar, A.V.Ramaswamy, G.Pal-Borbely: Catalysis Today, 75, 393-399 (2000).

(Received October 10, 2003; Accepted October 31, 2003)